RSC Advances

This is an *Accepted Manuscript*, which has been through the Royal Society of Chemistry peer review process and has been accepted for publication.

Accepted Manuscripts are published online shortly after acceptance, before technical editing, formatting and proof reading. Using this free service, authors can make their results available to the community, in citable form, before we publish the edited article. This *Accepted Manuscript* will be replaced by the edited, formatted and paginated article as soon as this is available.

You can find more information about *Accepted Manuscripts* in the Information for Authors.

Please note that technical editing may introduce minor changes to the text and/or graphics, which may alter content. The journal's standard Terms & Conditions and the Ethical guidelines still apply. In no event shall the Royal Society of Chemistry be held responsible for any errors or omissions in this *Accepted Manuscript* or any consequences arising from the use of any information it contains.

ROYAL SOCIETY OF CHEMISTRY

www.rsc.org/advances

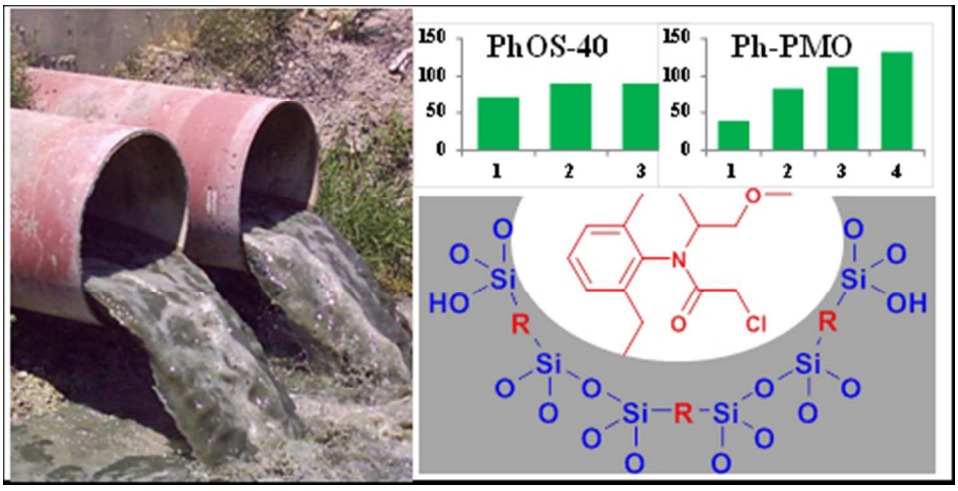

80x40mm (150 x 150 DPI)

RSC Advances Accepted Manuscript

Textual abstract

The adsorption of S-metolachlor on (organo)silicas largely depends on their composition and textural properties. Periodic mesoporous benzenesilica was particularly efficient for repetitive adsorption cycles.

RSC Advances Accepted Manuscript

Evaluation of different bridged organosilicas as efficient adsorbents for the herbicide S-metolachlor

María Isabel López,[a] Rocío Otero,[b] Dolores Esquivel,[a] César Jiménez-Sanchidrián,[a] José María Fernández,[b,*] and Francisco José Romero-Salguero[a,*]

[a] *Departamento de Química Orgánica, Instituto Universitario de Química Fina y Nanoquímica (IUQFN), Campus de Rabanales, Universidad de Córdoba, Campus de Excelencia Internacional Agroalimentario (ceiA3), Córdoba, Spain.*

[b] *Departamento de Química Inorgánica e Ingeniería Química, Instituto Universitario de Química Fina y Nanoquímica (IUQFN), Campus de Rabanales, Universidad de Córdoba, Campus de Excelencia Internacional Agroalimentario (ceiA3), Córdoba, Spain.*

* Corresponding authors.

Tel.: +34 957212065; fax: +34 957212066. E-mail address: qo2rosaf@uco.es (F. J. Romero-Salguero).

Tel.: +34 957218648; fax: +34 957580644. E-mail address: um1feroj@uco.es (J. M. Fernández).

RSC Advances Accepted Manuscript

Abstract

Three groups of porous non-ordered bridged organosilicas and silicas have been synthesized using three different surfactants of the Tween family as porogens. One group consisted in silica materials while the other two were organosilicas, i.e., ethanesilicas and benzenesilicas, but differing within each group in their textural properties. The adsorption of the herbicide S-metolachlor from an aqueous solution was then compared on all solids. The composition of the walls, i.e., the bridging group, was the main factor governing the adsorption capacity. Broadly, the uptake of the herbicide follows the sequence: benzenesilica > ethanesilica > silica. However, pore volume has also a significant influence on adsorption. Thus, higher capacities result from materials with larger pore volumes and with a larger size of the mesopores. Moreover, surface area and pore size distributions also affect the adsorption behavior, even though their influence seems to be less pronounced. Finally, a comparison between the porous non-ordered (organo)silicas and the corresponding periodic mesoporous (organo)silicas has revealed some interesting features for the use of these materials as adsorbents. Benzenesilicas with a large pore volume and pores in the micropore and/or large mesopore regions seemed to be the best adsorbents for adsorption in a single step whereas periodic mesoporous benzenesilicas were more appropriate for repetitive adsorptions.

Keywords: Organosilica, porous materials, adsorption, S-metolachlor, herbicides, water treatment.

RSC Advances Accepted Manuscript

1. Introduction

Bridged silsesquioxanes consist of organosilica networks prepared by hydrolysis and condensation of bis-silanes of the type $(R'O)_3Si\text{-}R\text{-}Si(OR')_3$. Usually, the bridge R is a relatively simple hydrocarbon unit such as a methylene, an ethylene or a phenylene group. Nevertheless, these bridges can also be of a high complexity.[1] Advantageously, all these groups are homogenously distributed along their structure. A particular case of these materials are periodic mesoporous organosilicas (PMOs).[2-4] They are synthesized in the presence of a surfactant template, thus giving rise to materials with long-distance ordering and pores in the meso range.[5, 6]

Both periodic mesoporous silicas and organosilicas have narrow pore size distributions in the mesoporous region (2-50 nm) and high surface areas. These properties make them good candidates for the adsorption of different molecules. Castricum et al.[7] described the application of microporous hybrid silica materials with alkylene and aromatic bridging groups of different sizes in membranes for the separation of gas mixtures such as H_2/N_2, CO_2/H_2 and CO_2/CH_4. The improved hydrothermal stability of hybrid structures has also provided membranes useful for water desalination.[8] In this sense, PMOs have been proven to be excellent adsorbents for organic compounds due to their improved hydrophobicity. Phenol derivatives,[9, 10] trinitrotoluene[11] and aromatic and polyaromatic hydrocarbons[12, 13] have been adsorbed on aliphatic and aromatic bridged PMOs. The combination of inorganic and organic moieties in their framework represented a real advantage even for the immobilization of enzymes.[14]

RSC Advances Accepted Manuscript

The presence of phenylene bridges is particularly advantageous when the adsorption of aromatic pollutants is concerned due to the pi–pi interactions between these compounds and the organosilica. Thus, a phenylene bridge led to a higher uptake of several phenol derivatives than an ethylene unit.[10] Similarly, the herbicide S-metolachlor was retained in a higher extent by a phenylene-bridged PMO than an ethylene-bridged PMO and a mesoporous silica.[15] The favorable presence of aromatic units in the pore walls was also proven for the relatively bulky pesticide mesosulfuron-methyl.[16] In this case, the introduction of sulfonic acid groups in the phenylene-bridged PMO enhanced the adsorption capacity via acid-base interactions with the NH group of the sulfonamide moiety in the pesticide. Very recently, a divinylaniline bridged PMO was employed for the removal of hexanal through a chemisorptive process.[17]

S-metolachlor is a pre- and post-emergence selective herbicide used to control grasses and some broad-leaved weeds in a wide range of crops. It is widely distributed in the environment and, in fact, 50.3% surface water sources and 2% of groundwater sources are contaminated with metolachlor in United States.[18, 19] Metolachlor is also one of the most relevant compounds contributing to Spanish groundwater contamination with concentrations above the environmental quality standard defined in the Directives 2006/118/EC and 2008/105/EC.[20] A similar situation has been found in other countries such as Greece[21] and Italy[22] in surface water and groundwater. Recent studies suggest that exposure to metolachlor results in decreased cell proliferation, growth and reproductive ability of non-target organisms.[23] The WHO Water Quality Criteria limits its concentration in 10.0 μg/L.

Herein, we report the synthesis of various silicas and organosilicas with different composition, i.e., nature of bridges, and textural properties using surfactants of the

RSC Advances Accepted Manuscript

Tween family, which were later used as adsorbents for the herbicide S-metolachlor. The relationship between the physicochemical properties of these materials and the pesticide uptake was analyzed and compared to that of the corresponding periodic mesoporous (organo)silicas.

2. Materials and methods

2.1. Materials

Three ordered materials, i.e., a periodic mesoporous silica (PMS) and two organosilicas, namely ethane-PMO (E-PMO) and benzene-PMO (Ph-PMO), were synthesized by using Brij-76 as surfactant under acidic conditions according to previously reported procedures.[24]

Non-ordered (organo)silicas were synthesized using tetraethyl orthosilicate (TEOS) (98%), 1,2-bis(triethoxysilyl)ethane (97%) and 1,4-bis(triethoxysilyl)benzene (96%), which were purchased from Acros, ABCR and Aldrich, respectively, as silica sources. The surfactants employed, all commercially available from Aldrich, were Tween 20 [polyoxyethylene(20)sorbitan monolaurate], Tween 40 [polyoxyethylene(20)sorbitan monopalmitate] and Tween 60 [polyoxyethylene(20)sorbitan monostearate]. HCl (37%) and ethanol (96% v/v), used to remove the surfactant, were provided by Panreac. NH_4F (≥98.0%), used as catalyst, was acquired from Sigma-Aldrich. All these chemicals were used without further purification.

The synthesis of the non-ordered materials was performed following a similar procedure to that described in a previous work for silicas.[25] In brief, 184 mmol of TEOS

RSC Advances Accepted Manuscript

or 92 mmol of organodisilane, i.e., 1,2-bis(triethoxysilyl)ethane or 1,4-bis(triethoxysilyl)benzene, were added dropwise to 184 mL of a solution that was 0.1 M in the corresponding surfactant (Tween 20, 40 or 60) and 0.02 M in the catalyst (NH_4F). After stirring for 24 h at room temperature, the formed precipitate was aged for 5 days at room temperature. Finally, the resulting solid was filtered, washed with 300 mL of distilled water and dried in the air.

The surfactant was removed by refluxing the as-synthesized material in an HCl solution (1 mL of 37% HCl in 50 mL of ethanol, per gram of solid) for 12 h. Subsequently, the solid was filtered and washed with ethanol. This process was repeated twice. The final material was then dried in a drying chamber at 100 ºC under vacuum.

The non-ordered materials, i.e, silica, ethanenesilica and benzenesilica, were named as S, EOS and PhOS, followed by a number denoting the surfactant used, that is, 20, 40 and 60 for Tween 20, Tween 40 and Tween 60, respectively.

Analytical standard S-metolachlor (2-chloro-N-(2-ethyl-6-methylphenyl)-N-[(1S)-2-methoxy-1-methylethyl] acetamide) was supplied by Sigma Aldrich. Its water solubility at 25 ºC is 480 mg/L.

2.2. Characterization

All hybrid materials were characterized by different techniques. X-ray powder diffraction (XRD) patterns were recorded on a Siemens D-5000 powder diffractometer (Cu-Kα radiation). N_2 isotherms were determined on a Micromeritics ASAP 2010 analyzer at -196 ºC. The specific surface area of each solid was determined using the BET method over a relative pressure (P/P_0) range of 0.05-0.20 and the pore size distribution was obtained by analysis of the adsorption branch of the isotherms using the

RSC Advances Accepted Manuscript

Barrett-Joyner-Halenda (BJH) method. Prior to the measurements, the samples were outgassed at 120 ºC for 24 h. A 3Flex equipment from Micromeritics was used for two samples. In this case, the porosity distribution was determined by a density functional theory (DFT) method using a cylindrical model for N_2 on an oxide surface. Particle size data were obtained in a Mastersizer S particle size analyzer by laser diffraction technology with a small volume dispersion unit of Malvern Instruments. Before the measurements, the samples were dispersed in distilled water and sonicated for 10 min. TEM micrographs were taken using a JEOL JEM 1400 instrument on samples supported on copper grids with carbon coating. ^{29}Si MAS NMR spectra were recorded at 79.49 MHz on a Bruker Avance 400 WB dual channel spectrometer at room temperature. An overall of 1000 free induction decays were accumulated. The excitation pulse and recycle time were 6 μs and 60 s, respectively. Chemical shifts were measured relative to tetramethylsilane standard. Before analysis, the samples were dried at 150 ºC for 24 h. Deconvolution of the spectra were performed with PeakFit software. The variation of zeta potential with pH was determined using Laser Doppler Velocimetry implemented in a Malvern Zetasizer Nano ZS equipped with a MPT-2 autotitrator. UV spectroscopy (Perkin Elmer UV-visible spectrophotometer, Model Lambda 11) at 265 nm was used to determine the concentration of S-metolachlor.

2.3. Adsorption experiments

S-Metolachlor adsorption on mesoporous materials was studied suspending in triplicate samples of 20 mg of each adsorbent in 30 mL of aqueous herbicide solution (100.0 mg/L) with an initial pH value of 2 (for the silica and ethanesilica samples) or 4 (for the benzenesilica samples).[15] Samples of adsorbent and herbicide in water were

RSC Advances Accepted Manuscript

shaken in a turn-over shaker at 52 rpm for 24 h. Adsorption kinetics was carried out at different contact times (Figure S1). Then, the supernatant liquid was centrifuged and separated to determine the concentration of S-metolachlor by UV-Vis spectroscopy (Figure S2). The amounts of adsorbed herbicide were determined from the initial and final solution concentrations.

Successive adsorptions were carried out by suspending the solid (adsorbent-herbicide) in 30 mL of a fresh aqueous herbicide solution (100.0 mg/L). The contact time was 24 h. After shaking, the suspensions were centrifuged and the herbicide concentration determined by UV-Vis spectroscopy. The charged material was used again for a new adsorption cycle up to completion of 4 successive adsorptions. The regeneration of the adsorbent was performed in ethanol with 30 ml of extracting volume and 24 h of contact time.

3. Results and discussion

3.1. (Organo)silicas as adsorbents for S-metolachlor

Different silicas, ethanesilicas and benzenesilicas have been synthesized using three different Tween surfactants as porogens (Scheme 1). The integrity of the organic bridges was verified by FT-IR measurements (Figure S3).[26] Thus, bands at 1277, 1414, 2899 and 2986 cm^{-1} corresponded to vibrations of the CH_2 groups in ethane bridges. Benzene bridges showed the C-H and C-C vibrations at 3069, and 1461 and 1636 cm^{-1}, respectively. Furthermore, intense bands between 1000 and 1110 cm^{-1} assigned to Si-O vibrations could be observed in all (organo)silicas.

RSC Advances Accepted Manuscript

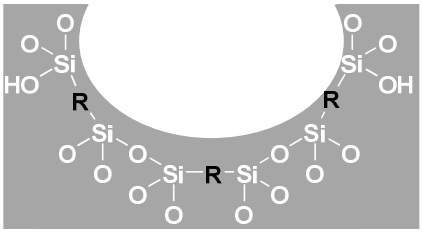

Scheme 1 Schematic representation of a pore for the different materials synthesized. R = -O-, -C_2H_4- or -C_6H_4- for silicas, ethanesilicas and benzenesilicas, respectively. The shaded area represents the wall of the material.

XRD analyses (Fig. S4) revealed that all these materials were non-periodic, that is, they lacked long distance ordering. Nevertheless, all of them exhibited high specific surface areas and pore volumes (Table 1). Their N_2 adsorption-desorption isotherms were of type IV with hysteresis loops exhibiting different shapes (Fig. 1). Therefore, even though all these materials had pores in the meso range, their porosity showed significant differences. In fact, all these adsorbents contained pores over a wide range of sizes. Samples S-20 and S-40 displayed a step at a relative pressure of 0.4-0.6 and a hysteresis loop of type H2, typical of disordered mesoporous systems.[26] Their pore size distribution curves indicated the existence of pores in the mesopore range at ca. 4 and 5 nm, respectively (Fig. 2). Material EOS-60 also had pores around 4 nm, although the step was hardly observed. In some cases, the adsorption step was shifted to high relative pressures (>0.6) by the effect of the increase in pore size, which was the case for solid S-60 with mesopores around 7 nm. On the contrary, materials EOS-20 and EOS-40 did not show any hysteresis loop at $P/P_0<0.8$ because the step occurred at quite low relative pressure, thus resulting in pores in the low mesopore range (<3 nm). Furthermore,

RSC Advances Accepted Manuscript

material PhOS-20 exhibited a type H4 loop, which is usually ascribed to slit-shaped pores in the micropore range.[27] The presence of a separate hysteresis loop above P/P_0 = 0.8 for several samples (i.e., S-40 and EOS-60) was suggestive of textural porosity, which represents the void space between randomly packed elementary particles, in the large meso and macropore range. As can be observed, several samples (i.e., S-60 and PhOS-40) exhibited different overlapped hysteresis loops, thus suggesting a combination of different porous systems. Clearly, the use of different surfactants of the Tween family gave rise to important differences within each group. Most of the samples exhibited mesopores with diameters above 10 nm and/or macropores, even though those materials prepared from Tween 20 mainly had small mesopores and/or micropores.

Periodic mesoporous silica (PMS) and organosilicas (ethane-PMO and benzene-PMO) were previously shown to exhibit isotherms of type IV typical of mesoporous materials with a narrow pore size distribution.[15] Among the non-ordered porous materials, only those synthesized in the presence of surfactant Tween 20 presented an analogous pore size distribution to PMS and PMOs, even though it was shifted to smaller pore sizes for PhOS-20 than for Ph-PMO.

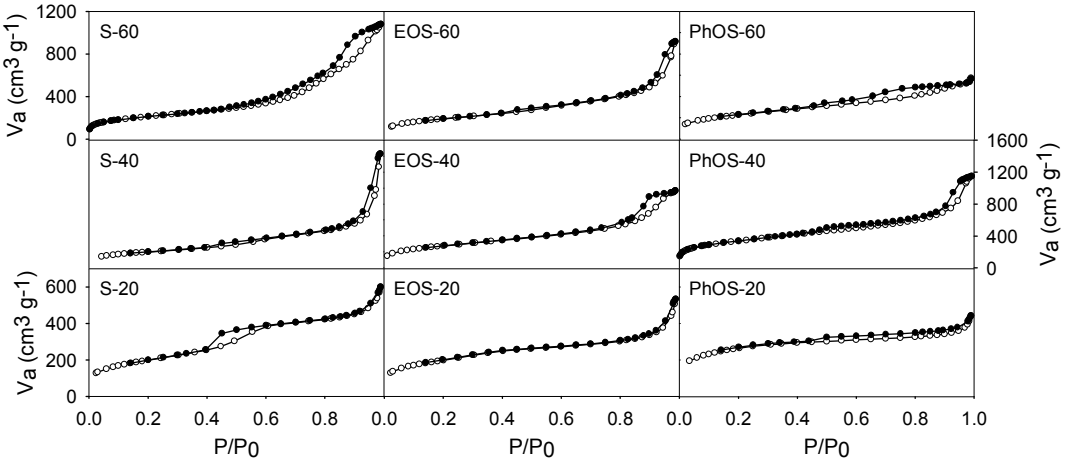

Fig. 1 Nitrogen adsorption-desorption isotherms for non-ordered porous (organo)silicas.

RSC Advances Accepted Manuscript

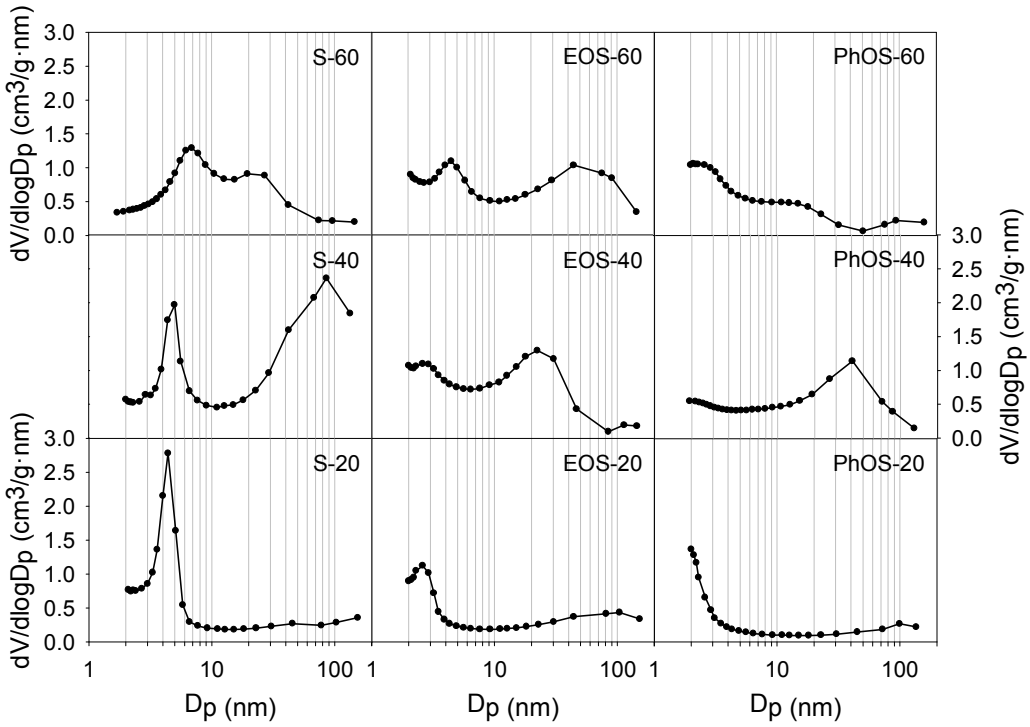

Fig. 2 Pore size distribution curves for non-ordered porous (organo)silicas.

Table 1 Physicochemical properties of non-ordered porous (organo)silicas and periodic mesoporous (organo)silicas.

Material	S_{BET} [a] ($m^2\ g^{-1}$)	V_p [b] ($cm^3\ g^{-1}$)	S_{micro} [c] ($m^2\ g^{-1}$)
S-20	723	0.81	47
S-40	721	1.39	52
S-60	746	1.67	92
PMS	885	1.17	0
EOS-20	715	0.68	84
EOS-40	994	1.44	84
EOS-60	697	1.19	21
E-PMO	1059	1.00	26
PhOS-20	942	0.58	250
PhOS-40	1160	1.69	111
PhOS-60	824	0.81	48
Ph-PMO	986	0.72	161

[a] BET specific surface area determined in the range of relative pressures from 0.05 to 0.20; [b] Single point total pore volume of pores; [c] Micropore area determined by t-plot method.

RSC Advances Accepted Manuscript

The transmission electron micrographs (Fig. 3) clearly reflected the existence of small elementary particles forming larger porous aggregates, which is consistent with the textural porosity apparent from the nitrogen adsorption–desorption isotherms. Also, in agreement with their isotherms, silica materials exhibited highly disordered pores in the meso range (4-5 nm). Although less evident, pores with sizes around 3-4 nm were also observable in ethanesilicas. Higher magnification images were in good agreement with the pore sizes determined by N_2 adsorption (Fig. 2).

The porous network of fused particles, particularly for silica samples, packed more densely in the following order of surfactants: Tween 20 > Tween 40 ≥ Tween 60, thus resulting in more uniform pore systems when using the former. In the case of benzenesilicas, the pores in sample PhOS-20 were hardly observable because they fell in the microporous range.

RSC Advances Accepted Manuscript

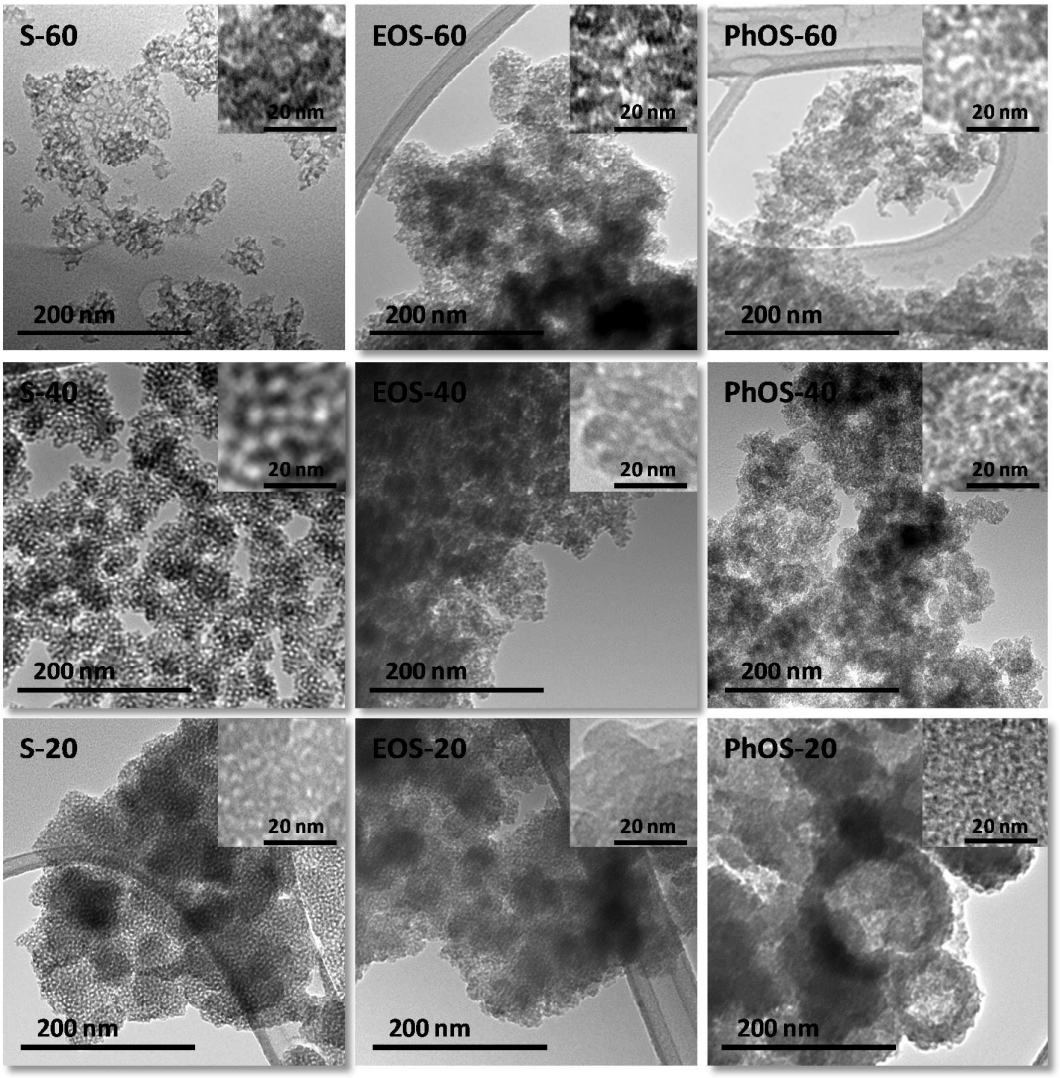

Fig. 3 TEM images for non-ordered porous (organo)silicas.

The different (organo)silicas exhibited the particle size distribution curves depicted in Fig. 4. In general, wide distributions in particle size were observed in all cases, even though silicas presented narrower size distributions than organosilicas. Within each group, the particle size seemed to be dependent on the surfactant used as porogen. Thus, it increased in the following order: Tween 20 < Tween 60 < Tween 40. Moreover, those (organo)silicas synthesized in the presence of Tween 20 surfactant

RSC Advances Accepted Manuscript

displayed a narrower particle size distribution. In this case, the particle size decreased in the order PhOS-20 < EOS-20 < S-20. Also, the particle size distribution curves for the corresponding PMOs are given as a reference.

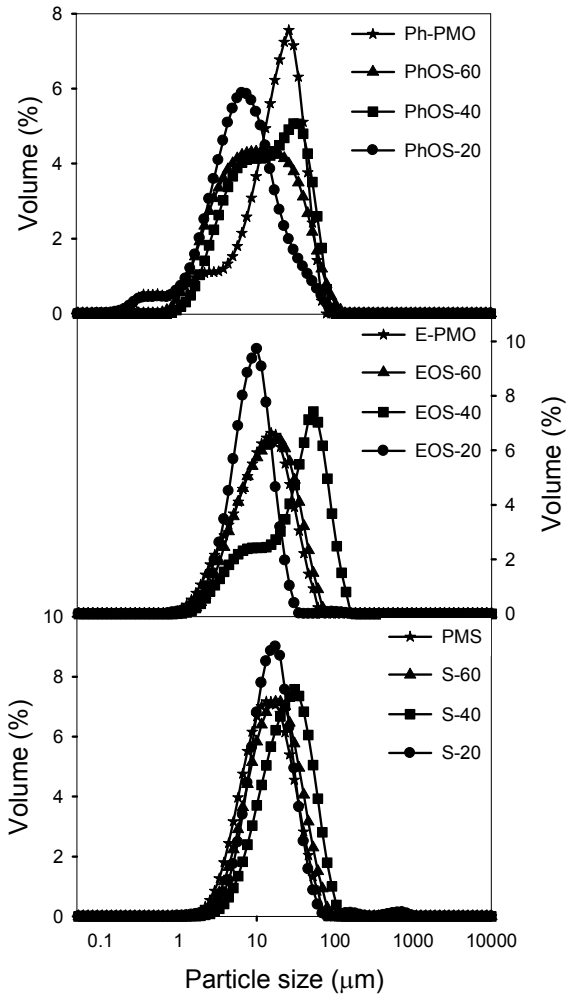

Fig. 4 Particle size distribution curves for non-ordered porous (organo)silicas and periodic mesoporous (organo)silicas.

All the silicas and organosilicas were used as adsorbents for the removal of S-metolachlor from water. The adsorption experiments for silicas and ethane-PMOs were carried out at pH=2, whereas those for benzenesilicas were done at pH=4, according to

RSC Advances Accepted Manuscript

the behavior previously observed in PMOs.[15] The amount of adsorbed herbicide in the three groups of materials revealed significant differences among them (Fig. 5). Broadly, as expected, the composition of the adsorbent, that is, the nature of the bridge, was decisive. The adsorption capacity toward the herbicide S-metolachlor was higher for benzenesilicas, followed by ethanesilicas and finally by silicas. Unlike silicas and ethanesilicas, all benzenesilicas adsorbed herbicide. The importance of the aromaticity in the adsorption of this non-ionic herbicide has also been evidenced for other very different adsorbents, as was the case for maize mulch residues exposed to microbial decomposition, whose capacity corresponded to the lignin fraction.[28] However, significant differences could be observed for different materials within the same group, that is, with the same composition. Obviously, within each group, an increase in the surface area of the materials would benefit to the uptake of S-metolachlor because the area of interaction between the (organo)silicas and the herbicide would be more extensive. However, although the materials with the largest surface gave the highest uptakes, some results could not be properly explained. Thus, sample EOS-60 had a slightly lower surface area than sample EOS-20, but the former adsorbed much more herbicide than the latter.

Apparently, the main factor governing the adsorption capacity within each group was the pore volume. Thus, the larger the pore volume, the higher the adsorption capacity was for both silica and organosilicas. This explained the differences between samples EOS-60 and EOS-20. By comparing the herbicide uptake for S-60, EOS-40 and PhOS-40, which were those materials with the highest pore volumes within each group, a higher efficiency of the organosilicas, particularly the benzenesilica, than the silica was observed. However, the distribution of pore size must affect the herbicide uptake because otherwise it is not possible to explain the significant differences among them.

RSC Advances Accepted Manuscript

Material PhOS-60 gave a lower herbicide uptake than sample PhOS-20, even though the former exhibited a higher pore volume. The significant difference between these two benzenesilicas seemed to be caused by the much higher micropore area in PhOS-20 than in PhOS-60. A comparison between samples S-60 and S-40 as well as between EOS-40 and EOS-60 suggested that a larger micropore area also favored the adsorption capacity of the adsorbent. Moreover, the best adsorbents within the silica and ethanesilica families, i.e., samples S-60 and EOS-40, respectively, displayed pores in the upper limit of the mesopores (18-30 nm) rather than macropores (>50 nm), apart from small mesopores. Indeed, sample PhOS-40 also exhibited an important fraction of pores at ca. 40 nm.

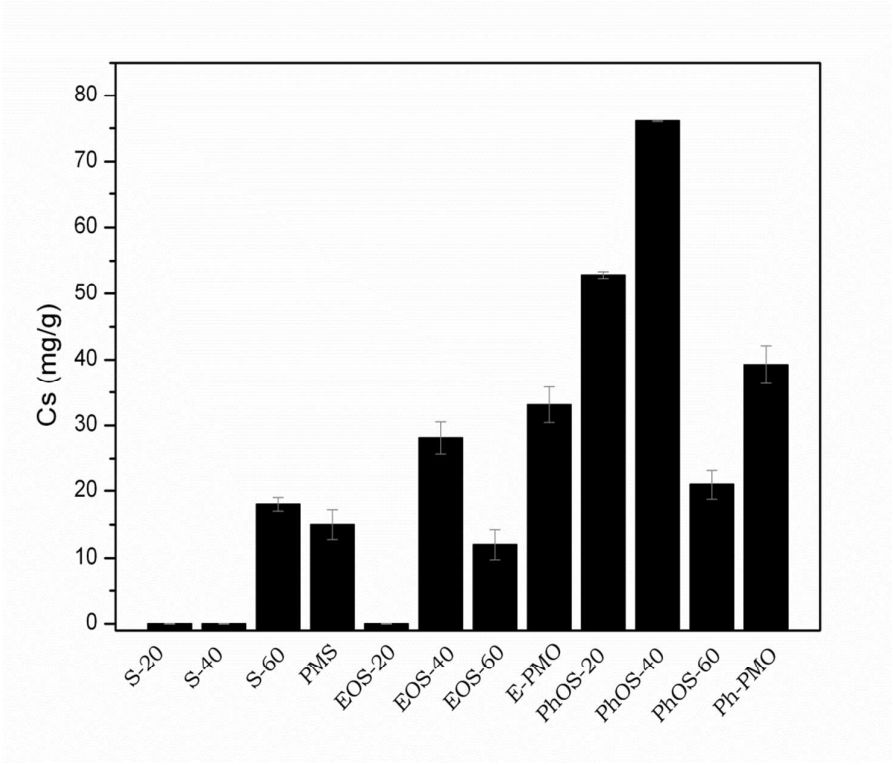

Fig. 5 Adsorption of S-metolachlor on non-ordered porous (organo)silicas and periodic mesoporous (organo)silicas.

RSC Advances Accepted Manuscript

Table 2 Adsorption capacities for S-metolachlor on different adsorbents.

Adsorbent	C_0 (mg/g) [a]	C_s (mg/g) [b]	Adsorption (%)	Ref.
Soils	0.08	0.04	50.0	[29]
Charcoals	400.0	136.2-156.0	36.5	[30]
Clays	158.9	56.8	37.8	[31]
Organohydrotalcites (OHTs)	149.0	79.7	53.5	[32]
PMS	149.0	15.0	10.1	[15]
E-PMO	149.0	36.0	24.2	[15]
	596.0	72.4	12.2	[15]
	532.1 (4 times) [c]	118.2	22.2	[15]
Ph-PMO	149.0	38.3	25.7	[15]
	596.0	189.3	31.8	[15]
	150.0 (4 times) [c]	133.6	89.1	This work
	532.1 (4 times) [c]	490.8	92.2	[15]
PhOS-40	150.0	76.1	50.7	This work
	150.0 (3 times) [c]	90.4	60.3	This work
Commercial carbon	150.0	117.9	78.6	[33]
	600.0	334.2	55.7	[33]
Mesoporous phenolic resin	150.0	94.3	62.9	[33]
	600.0	312.0	52.0	[33]
Mesoporous carbon	150.0	108.4	72.3	[33]
	600.0	347.1	57.9	[33]

[a] milligrams of herbicide in the starting solution per gram of adsorbent; [b] milligrams of herbicide adsorbed per gram of adsorbent; [c] number of adsorption cycles performed with the same material.

RSC Advances Accepted Manuscript

Benzenesilica PhOS-40 can be considered as an efficient adsorbent for S-metolachlor, with an uptake in the same range as some organohydrotalcites and charcoals, although lower than some microporous and mesoporous carbons (Table 2). Furthermore, the herbicide S-metolachlor can be completely desorbed from this benzenesilica by simple extraction with ethanol.

3.2. Comparison of a non-ordered porous benzenesilica with a periodic mesoporous benzenesilica as adsorbents for S-metolachlor

As previously stated, periodic mesoporous silica (PMS) and organosilicas (E-PMO and Ph-PMO) exhibited a good adsorption capacity within each family. Taking into account that the best adsorption behavior corresponded to benzenesilicas, we focused our study on materials PhOS-40 and Ph-PMO in order to ascertain the key factors influencing their differences in adsorption.

A previous study revealed that the aromatic π-π interactions prevailed for the adsorption of S-metolachlor on benzenesilica,[15] whereas electrostatic and hydrophobic interactions played an important role in silica and ethanesilica. Although PhOS-40 and Ph-PMO were synthesized starting from the same precursor, both materials were obtained under rather different conditions. Therefore, ^{29}Si MAS NMR spectra were registered in order to determine the hydroxylation degree in both samples (Fig. 6). Both materials exhibited practically identical composition of Si-OH groups. In fact, their condensation degrees and their number of OH groups per silicon atom were analogous (Table 3). Consequently, silanol groups cannot determine the different adsorption behavior of these materials.

RSC Advances Accepted Manuscript

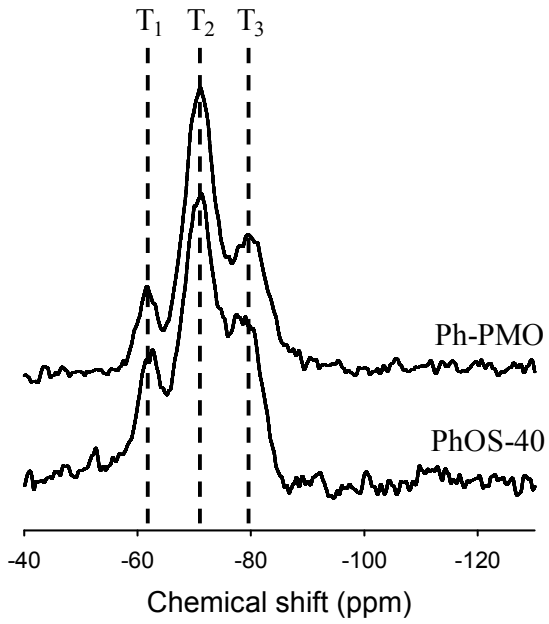

Fig. 6 ^{29}Si MAS NMR spectra for two benzenesilicas.

Table 3 ^{29}Si MAS NMR results obtained for two benzenesilicas.

Material	T_1 (%)	T_2 (%)	T_3 (%)	D (%) [a]	OH/ Si [b]
PhOS-40	17.1	50.3	32.6	72	0.85
Ph-PMO	13.3	57.1	29.6	72	0.84

[a] Condensation degree calculated from equation $D = [\Sigma(nT_n)\ ]/[(3 \times \Sigma T_n)\ )] \times 100$; [b] Content of silanol groups per silicon atom calculated from equation $OH/Si = (2T_1 + T_2)/(T_1 + T_2 + T_3)$.

Also, measurements of the variation of zeta potential with pH were carried out (Fig. 7). As observed, both materials showed very similar curves, thus indicating a similar surface charge, even though they were synthesized under different conditions. The point of zero charge (pzc) values for both materials were ca. 2.4, close to those reported for silica by other authors but lower than the value calculated by us following

RSC Advances Accepted Manuscript

the mass titration method.[15, 34, 35] Consequently, the disparities in the adsorption behavior for Ph-PMO and PhOS-40 cannot be attributed to differences in composition or surface charge.

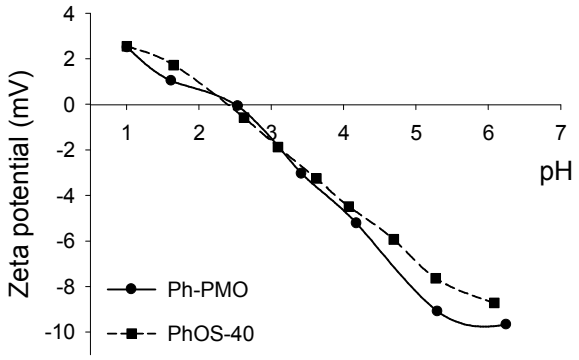

Fig. 7 Variation of zeta potential as a function of pH for two benzenesilicas.

Since the surface chemistry of both benzenesilicas was similar, the different adsorption capacity of these materials should be ascribed to their different textural properties. Again, the pore volume, which was much higher for PhOS-40 than for Ph-PMO, seemed to be decisive for the adsorption of the herbicide. A comparison of their pore size distribution curves (Fig. 8) determined by a DFT method showed clear differences between both solids. Ph-PMO mainly exhibited mesopores with a narrow distribution centered at ca. 4 nm as well as some micropores, whereas PhOS-40 had pores distributed in the whole size range with an important contribution of large mesopores.

RSC Advances Accepted Manuscript

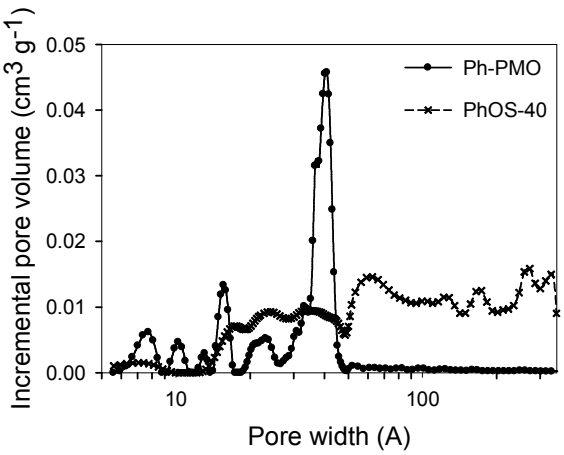

Fig. 8 Pore size distribution curves for two benzenesilicas.

A previously observed characteristic of Ph-PMO as adsorbent of S-metolachlor was its high capacity after successive adsorptions cycles (Table 2).[15] In fact, this material was able to retain herbicide up to saturation of its pore volume. This was attributed to the existence of phenylene bridges in its walls because ethylene bridges resulted in much less uptake and incomplete filling of pores. Thus, a comparison between Ph-PMO and PhOS-40 was done by subjecting them to four adsorption cycles (Fig. 9). Interestingly, PhOS-40 was saturated after only two successive adsorptions, whereas Ph-PMO was able to retain herbicide even after four adsorption cycles. At that point, Ph-PMO showed an uptake of 133.6 mg g^{-1} of S-metolachlor, thus still far from the maximum capacity reported for this material (490.8 mg g^{-1}).[15] Therefore, the high adsorption capacity of Ph-PMO has to be ascribed not only to the existence of aromatic bridges but also to its mesoporous character that allows to fill its whole pore volume.

RSC Advances Accepted Manuscript

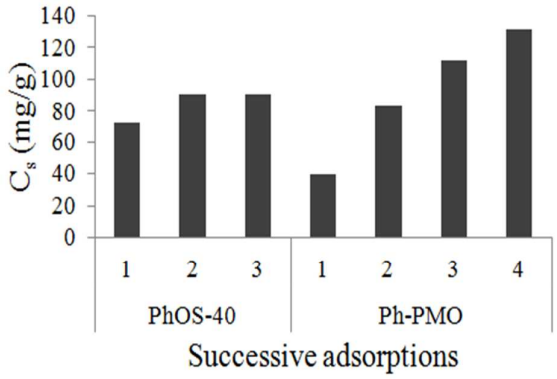

Fig. 9 Successive adsorptions of S-metolachlor for two benezenesilicas.

4. Conclusion

Various non-ordered porous (organo)silicas have been synthesized using Tween surfactants as porogens. They have been characterized and used as adsorbents for the herbicide S-metolachlor. A combination of several factors has been shown to determine the adsorption capacity of these materials. The main one was the chemical nature of the bridge. Thus, benzenesilicas gave the higher uptake, followed by ethanesilicas and finally by silicas. The surface area and particularly the pore volume were also proven to be essential for having a high uptake. Concerning the pore size distribution, those pores in the micropore and/or the large mesopore range seemed to be more favorable to adsorption. Clearly, the adsorption capacities of materials with different textural properties for organic molecules must be compared with caution.

The non-ordered materials were compared to the corresponding periodic mesoporous (organo)silicas. The use of the latter assured a good uptake in all cases unlike some of the non-ordered (organo)silicas. Interestingly, the phenylene-bridged

RSC Advances Accepted Manuscript

periodic mesoporous organosilica exhibited a higher capacity than the non-ordered benzenesilica after several successive adsorption cycles and therefore it would be the material of choice for multiple-pass adsorption processes.

Acknowledgements

The authors would like to thank Spanish Ministry of Economy and Competitiveness (Projects MAT2013-44463-R and CTM2011-25325), Junta de Andalucía (Project P10-FQM-6181 and Research Groups FQM-214 and FQM-346) and FEDER funds. M. I. L. and R. O. acknowledge Spanish Ministry of Education, Culture and Sport for their FPU research and teaching fellowships. The authors are greatly indebted to Micromeritics for measurements of the textural properties of samples PhOS-40 and Ph-PMO in a 3Flex equipment.

References

1. L. C. Hu and K. J. Shea, *Chem. Soc. Rev.*, 2011, **40**, 688.
2. S. Inagaki, S. Guan, Y. Fukushima, T. Ohsuna and O. Terasaki, *J. Am. Chem. Soc.*, 1999, **121**, 9611.
3. B. J. Melde, B. T. Holland, C. F. Blanford and A. Stein, *Chem. Mater.*, 1999, **11**, 3302.
4. T. Asefa, M. J. MacLachlan, N. Coombs and G. A. Ozin, *Nature*, 1999, **402**, 867.
5. F. Hoffmann, M. Cornelius, J. Morell and M. Fröba, *Angew. Chem. Int. Edit.*, 2006, **45**, 3216.
6. P. Van Der Voort, D. Esquivel, E. De Canck, F. Goethals, I. Van Driessche and F. J. Romero-Salguero, *Chem. Soc. Rev.*, 2013, **42**, 3913.
7. H. L. Castricum, G. G. Paradis, M. C. Mittelmeijer-Hazeleger, R. Kreiter, J. F. Vente and J. E. Ten Elshof, *Adv. Funct. Mater.*, 2011, **21**, 2319.
8. S. M. Ibrahim, R. Xu, H. Nagasawa, A. Naka, J. Ohshita, T. Yoshioka, M. Kanezashi and T. Tsuru, *RSC Adv.*, 2014, **4**, 23759.
9. M. C. Burleigh, S. Jayasundera, M. S. Spector, C. W. Thomas, M. A. Markowitz and B. P. Gaber, *Chem. Mater.*, 2004, **16**, 3.
10. M. C. Burleigh, M. A. Markowitz, M. S. Spector and B. P. Gaber, *Environ. Sci. Technol.*, 2002, **36**, 2515.

RSC Advances Accepted Manuscript

11. S. A. Trammell, M. Zeinali, B. J. Melde, P. T. Charles, F. L. Velez, M. A. Dinderman, A. Kusterbeck and M. A. Markowitz, *Anal. Chem.*, 2008, **80**, 4627.
12. C. P. Moura, C. B. Vidal, A. L. Barros, L. S. Costa, L. C. Vasconcellos, F. S. Dias and R. F. Nascimento, *J. Colloid Interface Sci.*, 2011, **363**, 626.
13. C. B. Vidal, A. L. Barros, C. P. Moura, A. C. A. de Lima, F. S. Dias, L. C. G. Vasconcellos, P. B. A. Fechine and R. F. Nascimento, *J. Colloid Interface Sci.*, 2011, **357**, 466.
14. V. Gascón, I. Diaz, R. M. Blanco and C. Marquez-Alvarez, *RSC Adv.*, 2014, **4**, 34356.
15. R. Otero, D. Esquivel, M. A. Ulibarri, C. Jiménez-Sanchidrián, F. J. Romero-Salguero and J. M. Fernández, *Chem. Eng. J.*, 2013, **228**, 205.
16. S. O. Ganiyu, C. Bispo, N. Bion, P. Ferreira and I. Batonneau-Gener, *Micropor. Mesopor. Mater.*, 2014, **200**, 117.
17. S. Martens, R. Ortmann, F. J. Brieler, C. Pasel, Y. Joo Lee, D. Bathen and M. Fröba, *Z. Anorg. Allg. Chem.*, 2014, **640**, 632.
18. , ed. W. H. Organization, Second edition edn., 1996.
19. , ed. W. H. Organization, Geneva.
20. A. Jurado, E. Vàzquez-Suñé, J. Carrera, M. López de Alda, E. Pujades and D. Barceló, *Sci. Total Environ.*, 2012, **440**, 82.
21. T. A. Albanis, T. G. Danis and M. K. Kourgia, *Sci. Total Environ.*, 1994, **156**, 11.
22. R. Meffe and I. de Bustamante, *Sci. Total Environ.*, 2014, **481**, 280.
23. S. Hartnett, S. Musah and K. R. Dhanwada, *Chemosphere*, 2013, **90**, 1258.
24. M. C. Burleigh, S. Jayasundera, C. W. Thomas, M. S. Spector, M. A. Markowitz and B. P. Gaber, *Colloid Polym. Sci.*, 2004, **282**, 728.
25. M. a. A. Aramendía, V. Borau, C. Jiménez, J. M. Marinas and F. J. Romero, *J. Colloid Interface Sci.*, 2004, **269**, 394.
26. J. E. S. S. Lowell, M. A. Thomas and M. Thommes, *Characterization of porous solids and powders: surface are, pore size and density*, Kluwer Academic Publishers, Dordrecht (The Netherlands), 2004.
27. J. R. F. Rouquerol, K. S. W. Sing, P. Llewellyn and G. Maurin, *Adsorption by powders and porous solids*, Second edition edn., Academic Press, Oxford, 2004.
28. S. Aslam, P. Garnier, C. Rumpel, S. E. Parent and P. Benoit, *Chemosphere*, 2013, **91**, 1447.
29. Y. Si, K. Takagi, A. Iwasaki and D. Zhou, *Pest. Manag. Sci.*, 2009, **65**, 956.
30. M. Bosetto, P. Arfaioli and P. Fusi, *Sci. Total Environ.*, 1992, **123**, 101.
31. A. Nennemann, Y. Mishael, S. Nir, B. Rubin, T. Polubesova, F. Bergaya, H. Van Damme and G. Lagaly, *Appl. Clay Sci.*, 2001, **18**, 265.
32. R. Otero, J. Fernández, M. Ulibarri, R. Celis and F. Bruna, *Appl. Clay Sci.*, 2012, **65**, 72.
33. R. Otero, D. Esquivel, M. A. Ulibarri, F. J. Romero-Salguero, P. Van Der Voort and J. M. Fernández, *Chem. Eng. J.*, 2014, **251**, 92.
34. J. S. Noh and J. A. Schwarz, *J. Colloid Interface Sci.*, 1989, **130**, 157.
35. J. Schwarz, C. Driscoll and A. Bhanot, *J. Colloid Interface Sci.*, 1984, **97**, 55.

RSC Advances Accepted Manuscript